 CMES, vol.49, no.2, pp.163-189, 2009

Energy-Conserving Local Time Stepping Based on High-Order Finite Elements for Seismic Wave Propagation Across a Fluid-Solid Interface

Ronan Madec[1], **Dimitri Komatitsch**[1,2] **and Julien Diaz**[3]

Abstract: When studying seismic wave propagation in fluid-solid models based on a numerical technique in the time domain with an explicit time scheme it is often of interest to resort to time substepping because the stability condition in the solid part of the medium can be more stringent than in the fluid. In such a case, one should enforce the conservation of energy along the fluid-solid interface in the time matching algorithm in order to ensure the accuracy and the stability of the time scheme. This is often not done in the available literature and approximate techniques that do not enforce the conservation of energy are used instead. We introduce such an energy-conserving local time stepping method, in which we need to solve a linear system along the fluid-solid interface. We validate it based on numerical experiments performed using high-order finite elements. This scheme can be used in any other numerical method with a diagonal mass matrix.

Keywords: Fluid-solid coupling, Time substepping, Seismic wave propagation, Spectral-element method.

1 Introduction

Coming along with the tremendous increase of computational power, the development of numerical methods for the accurate numerical simulation of the propagation of seismic waves in complex three-dimensional (3D) geological models has been the subject of a continuous effort in the last decades. Several numerical

[1] Université de Pau et des Pays de l'Adour, CNRS and INRIA Magique-3D. Laboratoire de Modélisation et Imagerie en Géosciences UMR 5212, Avenue de l'Université, 64013 Pau cedex, France. E-mail: ronan.madec@gmail.com, dimitri.komatitsch@univ-pau.fr

[2] Institut universitaire de France, 103 boulevard Saint-Michel, 75005 Paris, France.

[3] INRIA Magique-3D, Université de Pau et des Pays de l'Adour and CNRS. Laboratoire de Mathématiques et de leurs Applications UMR 5142, Avenue de l'Université, 64013 Pau cedex, France. E-mail: julien.diaz@inria.fr

approaches can be used to solve the equations of linear elastodynamics, for instance the finite-difference method (e.g., Alterman and Karal (1968); Madariaga (1976); Virieux (1986)), boundary-element (e.g., Kawase (1988)) or boundary-integral methods (e.g., Sánchez-Sesma and Campillo (1991)), spectral and pseudo-spectral methods (e.g., Tessmer and Kosloff (1994); Carcione (1994)), classical low-order finite-element methods (FEM) (e.g., Lysmer and Drake (1972); Bielak, Ghattas, and Kim (2005)), the spectral-element method (SEM) for regional (e.g., Liu, Polet, Komatitsch, and Tromp (2004)) or global (e.g., Chaljub, Komatitsch, Vilotte, Capdeville, Valette, and Festa (2007)) seismology, or discontinuous Galerkin formulations (e.g., Bernacki, Lanteri, and Piperno (2006); Käser and Dumbser (2006)).

In many cases of practical interest, for instance in deep offshore seismic studies in the oil industry, in ocean acoustics or in seismological studies of the Earth, which has a fluid outer core, fluid-solid models must been considered. Considering small deformation and non-moving fluid-solid interfaces is always sufficient in that context. Many of the above techniques can be extended to handle such fluid-solid models, for instance the finite-difference method (Virieux, 1986), the spectral-element method (Komatitsch, Barnes, and Tromp, 2000; Chaljub, Komatitsch, Vilotte, Capdeville, Valette, and Festa, 2007), or the discontinuous Galerkin formulation (Käser and Dumbser, 2008). The so-called 'grid method' (Zhang, 2004) can also be used. Another fruitful approach consists in coupling two different techniques at the fluid-solid interface, for instance a boundary-element method in the fluid and a finite-element method in the solid (Soares Jr. and Mansur, 2005) or finite elements and finite differences (Soares Jr., Mansur, and Lima, 2007). However using a boundary-element method in the fluid implies that the fluid is considered homogeneous, which is not feasible in the context of some applications such as ocean acoustics at long distance (in which the thermocline, i.e., wave speed variations, must be taken into account to model the SOFAR channel) or full Earth seismology (because in the fluid outer core of the Earth wave speed varies with radius).

In many of the above techniques a different formulation is used in each medium, for instance a formulation in displacement or in velocity and stress in the solid, and in pressure or in a potential in the fluid, and the two formulations are coupled along the fluid-solid interface. In the spectral-element method for instance coupling is enforced through a coupling integral along the fluid-solid interface (Komatitsch, Barnes, and Tromp, 2000; Chaljub, Komatitsch, Vilotte, Capdeville, Valette, and Festa, 2007). In the finite-difference method, which is not based on the weak form of the elastodynamics equations but rather on their strong form and on a staggered grid, one can set the shear wave speed to zero in the fluid (Virieux, 1986); however

van Vossen, Robertsson, and Chapman (2002) show that many grid points per shortest seismic wavelength are then needed to correctly model the Stoneley-Scholte interface wave at the ocean bottom when the ocean bottom is flat and aligned with a grid axis, and that the situation is even worse when non-flat bathymetry is present and/or when the ocean bottom is not aligned with a grid axis.

A key issue in the numerical modeling of fluid-solid models in the time domain is that it is often desirable to resort to time substepping because the stability condition in the solid part of the medium can be more stringent than in the fluid. This comes from the combination of two reasons:

- in many cases of practical interest, for instance in the oil industry, the value of the shear wave velocity at the ocean bottom on the solid side is similar to the value of the pressure wave velocity on the fluid side (in the ocean) and thus a spatially conforming mesh is needed to keep a similar mesh resolution,
- but the maximum pressure wave speed, which governs the stability condition of explicit time schemes, is often much higher in the solid than in the fluid, which is often water; the ratio can typically be between 2 and 5.

Therefore, being able to use a significantly larger time step on the fluid side is useful in order to save computational time. Several schemes or approximations are available in the literature to do that, for instance Casadei and Halleux (2009) and references therein, or Soares Jr., Mansur, and Lima (2007) in the context of finite difference-finite element coupling. Time substepping is also sometimes used in the context of fluid-fluid (e.g., Diaz and Grote (2009); Soares Jr. (2009)) or solid-solid (e.g., Tessmer (2000); Kang and Baag (2004); Dumbser, Käser, and Toro (2007)) models in which at least one region has much higher pressure wave velocities and/or much smaller mesh cells, i.e., a very restrictive stability limit, for instance to study the interaction of tube waves with cracks in oil wells, or when very low shear wave velocities are present for instance in the weathered zone in oil and gas industry models (Tessmer, 2000). Time substepping can also be of interest to study other systems numerically, for instance the advection-diffusion equation (El Soueidy, Younes, and Ackerer, 2009).

At an interface across which the time step changes, energy conservation should be ensured along the interface, otherwise instabilities and/or inaccuracies can arise. But this is often not done in the available literature and approximate techniques that do not enforce the conservation of energy are used instead. For instance Tessmer (2000) does not explicitly enforce energy conservation and observes that small spurious reflected and refracted waves arise in his snapshots of wave propagation. In the case of fluid-solid coupling, one should therefore enforce the conservation

of energy along the fluid-solid interface in the time-marching algorithm in order to ensure the accuracy and the stability of the time scheme. Some classical time integration schemes ensure the conservation of energy inside a given domain, see e.g. Simo, Tarnow, and Wong (1992); Tarnow and Simo (1994), Cohen (2002) (p. 142), Kane, Marsden, Ortiz, and West (2003); Collino, Fouquet, and Joly (2003a,b); Hairer, Lubich, and Wanner (2006); Nissen-Meyer, Fournier, and Dahlen (2008); Celledoni, McLachlan, McLaren, Owren, Quispel, and Wright (2009). But when coupling two different domains in a non conforming fashion (in time or in space) one must in addition enforce the conservation of total energy along the interface explicitly. In this article we therefore introduce such an energy-conserving local time stepping method, which is both accurate and numerically stable. To implement it we need to solve a linear system along the fluid-solid interface. We validate it based on numerical experiments performed using a spectral-element method and check that energy conservation along the fluid-solid interface is ensured from a numerical point of view.

2 Brief description of the classical fluid-solid coupling technique with no sub-stepping

Let us consider an acoustic fluid and an elastic solid in contact. We consider a linear elastic rheology for the solid, while the fluid is assumed to be inviscid. In the heterogeneous, elastic region the linear seismic wave equation can be written in the strong form as:

$$\rho \ddot{\mathbf{u}}_s = \nabla \cdot (\mathbf{c} : \nabla \mathbf{u}_s), \tag{1}$$

where $\mathbf{u}_s$ denotes the displacement vector in the solid, $\mathbf{c}$ the fourth-order stiffness tensor, and ρ the density. A dot over a symbol indicates time differentiation and the colon represents a double tensor contraction operation. The wave field in the heterogeneous, acoustic, inviscid fluid is governed by the conservation and dynamics equations which, neglecting the effects of gravity, are:

$$\begin{aligned} \rho \ddot{\mathbf{u}}_f &= -\nabla p, \\ p &= -\kappa (\nabla \cdot \mathbf{u}_f), \end{aligned} \tag{2}$$

where $\mathbf{u}_f$ denotes the displacement vector in the fluid, p denotes pressure and κ is the bulk modulus of the fluid. The displacement in the fluid can be described based on a potential ϕ defined by $\nabla \phi = \rho \mathbf{u}_f$.

To couple the two media at a fluid-solid interface, we have to ensure the continuity of the traction vector and of the normal component of the displacement vector.

In this article we solve the above seismic wave equation in the coupled fluid-solid medium based on a Legendre spectral-element method, as for instance in

Komatitsch, Barnes, and Tromp (2000), Komatitsch and Tromp (2002) or Chaljub, Komatitsch, Vilotte, Capdeville, Valette, and Festa (2007), i.e., we rewrite the equations of motion (1) and (2) in a weak form, using the potential ϕ above as unknown in the fluid. On the edges of the domain we use a free surface (i.e., zero traction) boundary condition. In the solid this condition is easily implemented in the weak formulation since the integral of traction along the boundary simply vanishes (e.g., Komatitsch and Vilotte (1998)). In the fluid the condition needs to be imposed explicitly by setting pressure, or equivalently the potential ϕ, to zero for the grid points that lie on the edges of the domain.

As is traditional for the spectral-element method (see e.g. Chaljub, Komatitsch, Vilotte, Capdeville, Valette, and Festa (2007)), temporal discretization is based on a non iterative explicit Newmark scheme, i.e., a central finite-difference scheme, which is conditionally stable and therefore the maximum value of the time step is defined by the Courant-Friedrichs-Lewy (CFL) stability condition (see e.g. Newmark (1959); Hughes (1987)). That scheme preserves momentum (Simo, Tarnow, and Wong, 1992) and also conserves our definition of discrete energy (11) and the so-called 'equivalent energy' (Krenk, 2006). Other (slightly different) definitions of discrete energy slightly oscillate, but around a mean value that is preserved (Kane, Marsden, Ortiz, and West, 2003; Krenk, 2006).

Let us write the spectral-element discretization of the variational formulation of the seismic wave equation above in the solid medium as a matrix system (e.g., Komatitsch and Vilotte (1998)), and in order to do so let us denote U, V and A the global displacement, velocity and acceleration vectors of unknowns, respectively, M the diagonal mass matrix and K the stiffness matrix:

$$\left\{ \begin{array}{l} U^{n+1} = U^n + \Delta t V^n + \frac{\Delta t^2}{2} A^n \\ V^{n+1/2} = V^n + \frac{\Delta t}{2} A^n \\ M A^{n+1} = K U^{n+1} \\ V^{n+1} = V^{n+1/2} + \frac{\Delta t}{2} A^{n+1} \end{array} \right. \tag{3}$$

Let us also write the spectral-element discretization of the variational formulation of the seismic wave equation in the fluid medium as a matrix system and introduce coupling terms to enforce the continuity of the traction vector and of normal displacement on the fluid-solid interface (e.g., Komatitsch, Barnes, and Tromp (2000); Komatitsch and Tromp (2002)); if we denote Φ the global vector of unknowns corresponding to the potential ϕ in the fluid defined above, $\dot{\Phi}$ and $\ddot{\Phi}$ its first and second time derivatives, and if we use a conforming time-stepping scheme for now, i.e., the

same time step $\Delta t_s = \Delta t_f = \Delta t$ everywhere, this gives:

$$\begin{cases} U^{n+1} = U^n + \Delta t V^n + \frac{\Delta t^2}{2} A^n \\ V^{n+1/2} = V^n + \frac{\Delta t}{2} A^n \\ M_s A^{n+1} = K_s U^{n+1} - B\ddot{\Phi}^{n+1} \\ V^{n+1} = V^{n+1/2} + \frac{\Delta t}{2} A^{n+1} \end{cases} \tag{4}$$

and

$$\begin{cases} \Phi^{n+1} = \Phi^n + \Delta t \dot{\Phi}^n + \frac{\Delta t^2}{2} \ddot{\Phi}^n \\ \dot{\Phi}^{n+1/2} = \dot{\Phi}^n + \frac{\Delta t}{2} \ddot{\Phi}^n \\ M_f \ddot{\Phi}^{n+1} = K_f \Phi^{n+1} + B^* U^{n+1} \\ \dot{\Phi}^{n+1} = \dot{\Phi}^{n+1/2} + \frac{\Delta t}{2} \ddot{\Phi}^{n+1} . \end{cases} \tag{5}$$

B is the matrix representation of the coupling integral along the fluid-solid interface on the solid side and is therefore zero everywhere except for grid points that belong to the fluid-solid interface; B^* is the coupling matrix on the fluid side.

The above system is an explicit scheme, i.e., one can express all its unknowns at a given time step in terms of elements already computed at previous time steps and there is no need to invert any linear matrix system. Let us now see what happens when we introduce time substepping.

3 Description of the substepping technique

Let us show how we write a system with two different time steps without losing the conservation of energy along the fluid-solid interface. The ratio between the time steps in the two media (the fluid and the solid) must be a ratio of integers p/q. Rodríguez (2004) and Diaz and Joly (2005) applied this technique to a finite-element method written in velocity and pressure and discretized based on a leap-frog time scheme; here we write it for a formulation in displacement in the solid and in a potential in the fluid and discretize it based on a Newmark time scheme. For p time steps in the fluid and q time steps in the solid (i.e., $\Delta t_s/p = \Delta t_f/q = \Delta t$) we write:

$$\begin{cases} U^{pqn+ip} = U^{pqn+(i-1)p} + \Delta t_s V^{pqn+(i-1)p} + \frac{\Delta t_s^2}{2} A^{pqn+(i-1)p} \\ V^{pqn+(2i-1)\frac{p}{2}} = V^{pqn+(i-1)p} + \frac{\Delta t_s}{2} A^{pqn+(i-1)p} \\ M_s A^{pqn+ip} = K_s U^{pqn+ip} - B[\ddot{\Phi}]^{pqn+ip} \\ V^{pqn+ip} = V^{pqn+(2i-1)\frac{p}{2}} + \frac{\Delta t_s}{2} A^{pqn+ip} \end{cases} \tag{6}$$

and

$$\begin{cases} \Phi^{pqn+jq} = \Phi^{pqn+(j-1)q} + \Delta t_f \dot{\Phi}^{pqn+(j-1)q} + \frac{\Delta t_f^2}{2} \ddot{\Phi}^{pqn+(j-1)q} \\ \dot{\Phi}^{pqn+(2j-1)\frac{q}{2}} = \dot{\Phi}^{pqn+(j-1)q} + \frac{\Delta t_f}{2} \ddot{\Phi}^{pqn+(j-1)q} \\ M_f \ddot{\Phi}^{pqn+jq} = K_f \Phi^{pqn+jq} + B^* [U]^{pqn+jq} \\ \dot{\Phi}^{pqn+jq} = \dot{\Phi}^{pqn+(2j-1)\frac{q}{2}} + \frac{\Delta t_f}{2} \ddot{\Phi}^{pqn+jq} \end{cases} \tag{7}$$

for $i = 1,..,q$ and $j = 1,..,p$. The difficulty is to find a suitable approximation for the transmission terms at each local time step, $([U]^{pqn+jq})_{j=1,p}$ and $([\ddot{\Phi}]^{pqn+ip})_{i=1,q}$. Here and in all the following, variables between brackets represent terms that we cannot compute directly because the variables are not defined at this time index. The time discretization of these quantities will be chosen in a suitable fashion so as to ensure the conservation of energy along the fluid-solid interface. The important thing is to conserve global energy to ensure that the coupling substepping scheme be physically consistent and stable. After finding suitable approximations for the transmission terms, we can rewrite the system and find the implicit scheme that will permit the propagation for the local time step scheme. Let us illustrate this in the simple particular case $p/q = 1/2$.

3.1 Case of a 1/2 ratio

In this section, we impose $\Delta t_s = \Delta t_f/2 = \Delta t$. The coupled system can then be written the same way as in the conforming case:

First time step in the solid:

$$\begin{cases} U^{2n+1} = U^{2n} + \Delta t V^{2n} + \frac{\Delta t^2}{2} A^{2n} \\ V^{2n+1/2} = V^{2n} + \frac{\Delta t}{2} A^{2n} \\ M_s A^{2n+1} = K_s U^{2n+1} - B[\ddot{\Phi}]^{2n+1} \\ V^{2n+1} = V^{2n+1/2} + \frac{\Delta t}{2} A^{2n+1} \end{cases} \tag{8}$$

Second time step in the solid:

$$\begin{cases} U^{2n+2} = U^{2n+1} + \Delta t V^{2n+1} + \frac{\Delta t^2}{2} A^{2n+1} \\ V^{2n+3/2} = V^{2n+1} + \frac{\Delta t}{2} A^{2n+1} \\ M_s A^{2n+2} = K_s U^{2n+2} - B[\ddot{\Phi}]^{2n+2} \\ V^{2n+2} = V^{2n+3/2} + \frac{\Delta t}{2} A^{2n+2} \end{cases} \tag{9}$$

First and only time step in the fluid:

$$\begin{cases} \Phi^{2n+2} = \Phi^{2n} + 2\Delta t\dot{\Phi}^{2n} + 2\Delta t^2\ddot{\Phi}^{2n} \\ \dot{\Phi}^{2n+1} = \dot{\Phi}^{2n} + \Delta t\ddot{\Phi}^{2n} \\ M_f\ddot{\Phi}^{2n+2} = K_f\Phi^{2n+2} + B^*[U]^{2n+2} \\ \dot{\Phi}^{2n+2} = \dot{\Phi}^{2n+1} + \Delta t\ddot{\Phi}^{2n+2} \end{cases} \tag{10}$$

For such a system, the discrete energy in the solid and in the fluid is calculated as:

$$\begin{aligned} E_s^{2n} &= (M_sV^{2n+\frac{1}{2}}, V^{2n+\frac{1}{2}}) - (K_sU^{2n}, U^{2n+1}), \\ E_f^{2n} &= (M_f\ddot{\Phi}^{2n}, \ddot{\Phi}^{2n}) - (K_f\dot{\Phi}^{2n-1}, \dot{\Phi}^{2n+1}), \end{aligned} \tag{11}$$

where $(\cdot,\cdot)$ represents the scalar product. Total energy is defined as $E^{2n} = E_s^{2n} + E_f^{2n}$. These energies are positive if both time steps verify their respective CFL stability condition because K_f and K_s are definite negative by construction.

$$\begin{aligned} \frac{E^{2n+2} - E^{2n}}{2\Delta t} &= \frac{[U^{2n+2}] - [U^{2n}]}{2\Delta t} \times \frac{\dot{\Phi}^{2n+3} - \dot{\Phi}^{2n-1}}{4\Delta t} \\ -\frac{1}{2}\Big([\ddot{\Phi}^{2n+1}] &\times \frac{U^{2n+2} - U^{2n}}{2\Delta t} + [\ddot{\Phi}^{2n+2}] \times \frac{U^{2n+3} - U^{2n+1}}{2\Delta t}\Big) \end{aligned} \tag{12}$$

Ensuring energy conservation along the fluid-solid interface means finding $[\ddot{\Phi}]^{2n+1}$, $[\ddot{\Phi}]^{2n+2}$ and $[U]^{2n+2}$ such that $E^{2n+2} - E^{2n} = 0$, which implies that we must solve

$$\begin{aligned} \big([U]^{2n+2} - [U]^{2n}\big) \times \frac{\dot{\Phi}^{2n+3} - \dot{\Phi}^{2n-1}}{4\Delta t} - [\ddot{\Phi}]^{2n+1} \times \frac{U^{2n+2} - U^{2n}}{2} \\ - [\ddot{\Phi}]^{2n+2} \times \frac{U^{2n+3} - U^{2n+1}}{2} = 0. \end{aligned} \tag{13}$$

Taking

$$\ddot{\Phi}^{2n} = (\dot{\Phi}^{2n+1} - \dot{\Phi}^{2n-1})/2\Delta t \tag{14}$$

we solve (13) using

$$\begin{aligned} [U]^{2n+2} &= (U^{2n+3} + U^{2n+2})/2 \quad \text{and} \\ [\ddot{\Phi}]^{2n+2} &= [\ddot{\Phi}]^{2n+1} = (\ddot{\Phi}^{2n+2} + \ddot{\Phi}^{2n})/2. \end{aligned} \tag{15}$$

Now we simply need to replace the variables into brackets in (8-10) with (15) to obtain the following implicit system:

First time step in the solid:

$$\begin{cases} U^{2n+1} = U^{2n} + \Delta t V^{2n} + \frac{\Delta t^2}{2} A^{2n} \\ V^{2n+1/2} = V^{2n} + \frac{\Delta t}{2} A^{2n} \\ M_s A^{2n+1} = K_s U^{2n+1} - B \frac{\ddot{\Phi}^{2n+2} + \ddot{\Phi}^{2n}}{2} \\ V^{2n+1} = V^{2n+1/2} + \frac{\Delta t}{2} A^{2n+1} \end{cases} \tag{16}$$

Second time step in the solid:

$$\begin{cases} U^{2n+2} = U^{2n+1} + \Delta t V^{2n+1} + \frac{\Delta t^2}{2} A^{2n+1} \\ V^{2n+3/2} = V^{2n+1} + \frac{\Delta t}{2} A^{2n+1} \\ M_s A^{2n+2} = K_s U^{2n+2} - B \frac{\ddot{\Phi}^{2n+2} + \ddot{\Phi}^{2n}}{2} \\ V^{2n+2} = V^{2n+3/2} + \frac{\Delta t}{2} A^{2n+2} \end{cases} \tag{17}$$

First and only time step in the fluid:

$$\begin{cases} \Phi^{2n+2} = \Phi^{2n} + 2\Delta t \dot{\Phi}^{2n} + 2\Delta t^2 \ddot{\Phi}^{2n} \\ \dot{\Phi}^{2n+1} = \dot{\Phi}^{2n} + \Delta t \ddot{\Phi}^{2n} \\ M_f \ddot{\Phi}^{2n+2} = K_f \Phi^{2n+2} + B^* \frac{U^{2n+3} + U^{2n+2}}{2} \\ \dot{\Phi}^{2n+2} = \dot{\Phi}^{2n+1} + \Delta t \ddot{\Phi}^{2n+2} \end{cases} \tag{18}$$

We then rewrite the system to make each variable depend on $\ddot{\Phi}^{2n+2}$. This allows us to write a linear system:

$$C \ddot{\Phi}^{2n+2} = b^{2n+1}, \tag{19}$$

to be solved on the fluid-solid interface only, in which the unknown variable is $\ddot{\Phi}^{2n+2}$. Matrix C is defined as:

$$C = M_f + \Delta t^2 B M_s^{-1} B^* + \frac{\Delta t^4}{4} B M_s^{-1} K_s M_s^{-1} B^* \tag{20}$$

This matrix to invert is non-zero only for the grid points located on the fluid-solid interface, and the right-hand side b^{2n+1} depends on totally explicit variables plus the explicit part of the partially implicit variables (each variable has an explicit part and most variables also have an implicit part, as seen above). Matrix C does not vary with time and it can therefore be constructed and decomposed once and for all before the time loop. To improve computational efficiency we can therefore keep its LU decomposition and use it in the time loop to compute $\ddot{\Phi}^{2n+2}$.

After solving for $\ddot{\Phi}^{2n+2}$ on the interface, we inject it in the system (16-18) and we can then compute all the other unknowns of that time step.

3.2 Extension to the more general case of a p/q ratio

Let us now extend our method to the more general case of a p/q ratio of integers, such that $\Delta t_s/p = \Delta t_f/q = \Delta t$. The system to solve is then (6-7), in which discrete energy is defined as:

$$\begin{aligned} E_s^{pqn} &= (M_s V^{pqn+\frac{p}{2}}, V^{pqn+\frac{p}{2}}) - (K_s U^{pqn}, U^{pqn+p}), \\ E_f^{pqn} &= (M_f \ddot{\Phi}^{pqn}, \ddot{\Phi}^{pqn}) - (K_f \dot{\Phi}^{pqn-\frac{q}{2}}, \dot{\Phi}^{pqn+\frac{q}{2}}). \end{aligned} \tag{21}$$

To ensure energy conservation along the fluid-solid interface and therefore the stability of the scheme, we need to enforce that:

$$\begin{aligned} \frac{1}{p}\sum_{j=1}^{p}\Big(\big([U]^{pqn+jq} - [U]^{pqn+(j-1)q}\big) \times \frac{\dot{\Phi}^{pqn+(2j+1)\frac{q}{2}} - \dot{\Phi}^{pqn+(2j-3)\frac{q}{2}}}{2q\Delta t}\Big) \\ -\frac{1}{q}\sum_{i=1}^{q}\Big([\ddot{\Phi}]^{pqn+ip} \times \frac{U^{pqn+ip} - U^{pqn+(i-1)p}}{2}\Big) = 0, \end{aligned} \tag{22}$$

which leads to transmission terms $([U]^{pqn+jq})_{j=1,p}$ and $([\ddot{\Phi}]^{pqn+ip})_{i=1,q}$ for the system (6-7). One can show that (22) is ensured if the quantities into brackets verify the following sufficient conditions used by Rodríguez (2004):

$$\begin{aligned} &\forall i = 1,..,q-1, \qquad [\ddot{\Phi}]^{pqn+(i+1)p} = [\ddot{\Phi}]^{pqn+ip} \\ &\forall j = 1,..,p-1, \qquad [U]^{pqn+(j+1)q} - [U]^{pqn+jq} = [U]^{pqn+jq} - [U]^{pqn+(j-1)q}. \end{aligned} \tag{23}$$

This allows us to find a suitable solution to (22). For example, in the case of $p/q = 2/3$ (i.e., $p = 2$ and $q = 3$), the solution for the transmission terms is:

$$\begin{aligned} [U]^{6n+3} &= (U^{6n+8} + U^{6n+6} + U^{6n+2} + U^{6n})/4, \\ [U]^{6n+6} &= (U^{6n+8} + U^{6n+6})/2, \\ [\ddot{\Phi}]^{6n+6} &= [\ddot{\Phi}]^{6n+4} = [\ddot{\Phi}]^{6n+2} = (\ddot{\Phi}^{6n+6} + 2\ddot{\Phi}^{6n+3} + \ddot{\Phi}^{6n})/2. \end{aligned} \tag{24}$$

We can then build a linear system and solve (6-7). In the case of $p/q = 1/2$, we have already built that linear system around $\ddot{\Phi}^{2n+2}$ in (19). In the case of $p/q = 2/3$, the linear system would be built around $(\ddot{\Phi}^{6n+6} + 2\ddot{\Phi}^{6n+3})/2$.

4 Numerical tests

Let us now validate the time substepping approach by studying its accuracy and the time evolution of total discrete energy for two benchmarks previously studied by Komatitsch, Barnes, and Tromp (2000) in the conforming case, i.e., with the same time step in the fluid and in the solid.

4.1 Flat interface with $\Delta t_s = \Delta t_f/2$ or with $\Delta t_s = \Delta t_f \times 2/3$

The first test is for a flat fluid-solid interface. The model and the mesh are the same as in Komatitsch, Barnes, and Tromp (2000). The domain has a size of 6400 m $\times$ 4800 m and is meshed with 120×90 spectral elements, therefore each element has a size of 53.33 m $\times$ 53.33 m. In each spectral element we use polynomial basis functions of degree $N = 5$, i.e., each spectral element contains $(N+1)^3 = 216$ grid points. The fluid-solid interface is located at a depth of $z_{fs} = 2400$ m below the free surface of the fluid, i.e., in the middle of the model in the vertical direction (Figure 1). The upper layer is a fluid water layer with a compressional wave speed of 1500 m.s^{-1} and density of 1020 kg.m^{-3}; the lower layer is solid with a compressional wave speed of 3400 m.s^{-1}, a shear wave speed of 1963 m.s^{-1} and density of 2500 kg.m^{-3}. In order to be able to study the conservation of total discrete energy along the fluid-solid interface in our substepping technique we must not use absorbing conditions on the edges of the grid to mimic an infinite medium otherwise some energy would be absorbed and total energy would not remain constant with time. Instead we must study a closed medium. We therefore implement a free surface condition, which ensures total reflection of the waves, on the four sides of the mesh.

The source time function is the second derivative of a Gaussian (a so-called 'Ricker' wavelet) of dominant frequency 10 Hz located in the fluid at $x_s = 1575$ m at a depth of $z_s = 1900$ m, i.e., 500 m above the fluid-solid interface. A recording station (a receiver) is located in the fluid at $x_r = 3750$ m at a depth of $z_r = 1933.33$ m and records the time variation of the two components of the displacement vector in order to display a so-called 'seismogram' (i.e., the time history of a given component of the displacement vector at a given grid point). Since the seismic wave equation is linear, the amplitude of the source does not matter: multiplying the amplitude of the source by a certain factor simply means that the seismograms get multiplied by the same factor; therefore the actual amplitude of all the seismograms in what follows can be considered meaningless.

The dispersion and stability of the Legendre spectral-element method used in conjunction with an explicit conditionally-stable Newmark finite-difference time scheme have been studied for instance by Fauqueux (2003), De Basabe and Sen (2007) and Seriani and Oliveira (2008). Following Fauqueux (2003), the CFL stability limit for a regular mesh can be determined based on $c^p_{max}\Delta t/h \leq cfl_{1,5}/\sqrt{D}$, where c^p_{max} is the maximum pressure wave speed in a given layer of the model (1500 m.s^{-1} in the fluid and 3400 m.s^{-1} in the solid), Δt is the time step in the fluid or in the solid, h is the length of an edge of a mesh element (53.33 m here), D is the spatial dimension of the problem (2 here), and $cfl_{1,5}$ is the CFL stability limit in the 1D case for polynomial basis functions of degree $N = 5$ in space. Fauqueux (2003)

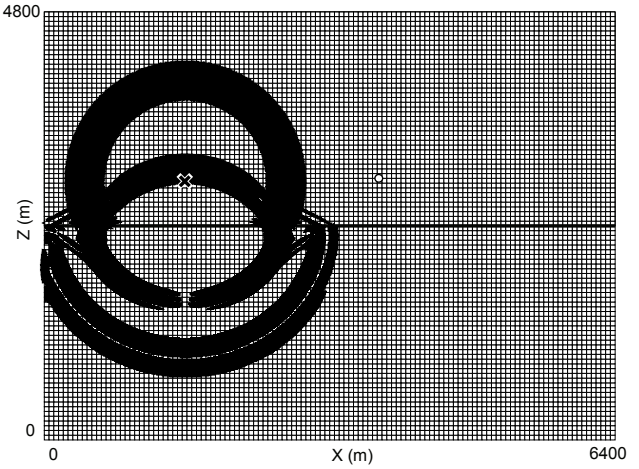

Figure 1: Mesh used for a flat ocean bottom with free surfaces on the four sides of the grid. The snapshot of the wave field superimposed is shown at time $t = 0.8816$ s and shows the pressure waves in the fluid upper layer and the pressure and shear waves in the solid lower layer. Each mesh cell has a size of 53.33 m $\times$ 53.33 m as in Komatitsch, Barnes, and Tromp (2000). The cross represents the position of the source and the circle indicates the position of the seismic receiver.

finds that a sufficient (but not necessary in the elastic case) limit (i.e., a slightly conservative estimate) is $cfl_{1,5} = 0.1010$; numerical tests that we performed to find the CFL limit experimentally showed us that we could go slightly higher (up to $cfl_{1,5} = 0.1014$) and we therefore determined that the CFL stability limit for our model is approximately $\Delta t_f = 2.53$ ms in the fluid and $\Delta t_s = 1.126$ ms in the solid.

Figure 2 (top) shows the seismogram recorded at the receiver in the case of conforming time stepping with a time step $\Delta t = 0.42$ ms and 5000 time steps in the fluid and in the solid, compared to the analytical solution computed based on the Cagniard-de Hoop technique using a computer program from Berg, If, Nielsen, and Skovegaard (1994). This figure therefore reproduces the results of Komatitsch, Barnes, and Tromp (2000). The fit between the numerical solution and the analytical solution is excellent. Figure 2 (bottom) shows the seismogram in the case of non conforming time steps with a p/q ratio of 1/2, i.e., $\Delta t_f = 2\Delta t_s = 0.42$ ms, i.e., for a time step in the solid that is about 1/5th of that of the CFL stability limit. We therefore perform 5000 time steps in the fluid and 10000 time steps in the solid. Again, we get an excellent fit between the numerical solution and the analytical solution, which shows the accuracy of the substepping technique.

In order to illustrate numerically the stability of the time substepping scheme, in

Figure 3 we study the evolution of the total discrete energy of the numerical scheme computed using (21) with $p = 1$ and $q = 2$. The source being located in the acoustic medium, energy is partially transferred to the elastic medium when the wave fronts (both the direct pressure wave front and the pressure wave front reflected off the free surface of the fluid layer) reach the fluid-solid interface, but the important thing to note is that total discrete energy is very well conserved.

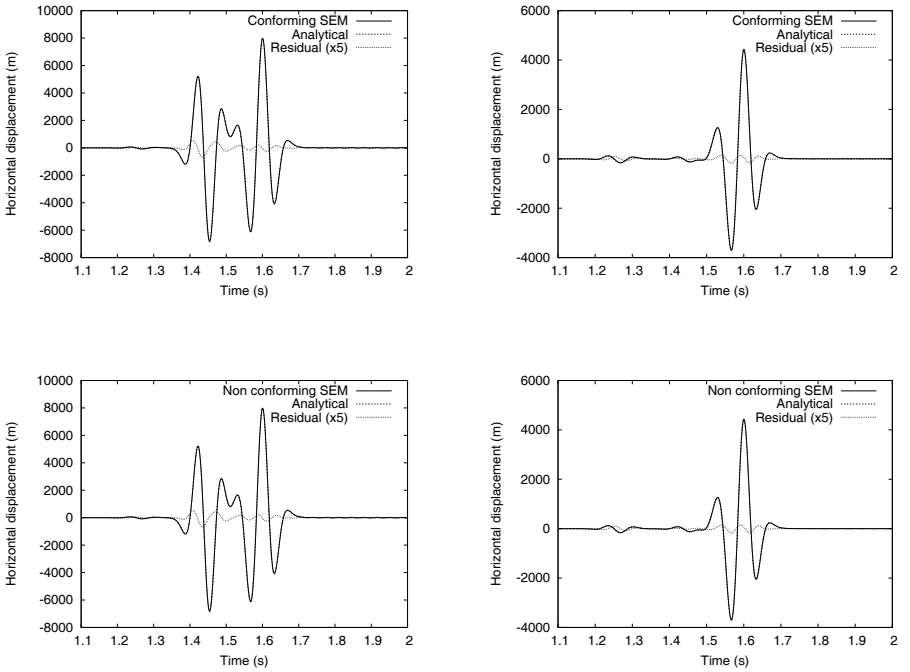

Figure 2: Comparison with the analytical solution from Berg, If, Nielsen, and Skovegaard (1994) (dashed line) of spectral-element seismograms (solid line) for the horizontal (left) and vertical (right) components of the displacement vector at the receiver located in the fluid for the model with a flat fluid-solid interface. The difference amplified by a factor of 5 is also shown (dotted line). (Top) The fit is excellent for conforming time stepping with $\Delta t_f = \Delta t_s = 0.42$ ms, i.e., at about CFL/5 in the fluid and CFL/2.5 in the solid. (Bottom) The fit is also excellent for non-conforming time stepping with $\Delta t_f = 0.42$ ms in the fluid and $\Delta t_s = 0.21$ ms in the solid, i.e., at about CFL/5 in both the fluid and the solid.

The above validation has been performed relatively far from the CFL stability limit (at about 1/5th of that limit). Let us now study what happens when we select a time step closer to the stability limit. For conforming time stepping, let us take

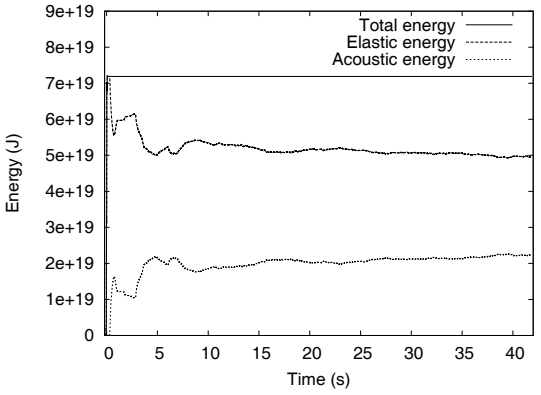

Figure 3: Time evolution of discrete energy in the fluid and in the solid as well as total discrete energy for the non conforming case with p/q = 1/2 for the model with a flat fluid-solid interface. We have $\Delta t_f = 2\Delta t_s = 0.42$ ms. We propagate the wave field for 100,000 time steps in the fluid and for 200,000 time steps in the solid. Total discrete energy is very well conserved.

$\Delta t = 1.125$ ms, which is very close to the CFL limit computed above and which is therefore the largest time step that we can select for our numerical tests in the conforming case. Figure 4 (top) shows that the fit to the analytical solution is not very good compared to Figure 2 (top). In the non conforming case with p/q = 1/2 and $\Delta t_f = 1.125$ ms in the fluid (Figure 4, bottom) we observe a similar poorer fit compared to the non conforming case with a smaller time step of Figure 2 (bottom). This shows that the main source of discrepancies is not the time substepping scheme but rather the numerical error (numerical dispersion) of the explicit Newmark finite-difference time scheme itself, which is only second-order accurate (Hughes, 1987) while the spatial polynomial basis functions that we have chosen for the spectral-element method are of degree $N = 5$. It would therefore be of interest to switch to higher-order time schemes such as fourth-order Runge-Kutta integration or symplectic schemes (e.g., Simo, Tarnow, and Wong (1992); Nissen-Meyer, Fournier, and Dahlen (2008)) for instance.

Finally, let us test the case of a p/q ratio equal to 2/3, i.e., $\Delta t_s = \Delta t_f \times 2/3$. We select $\Delta t_s = 0.28$ ms and $\Delta t_f = 0.42$ ms. Figure 5 shows that the fit to the analytical solution is very good, as in the case of p/q = 1/2 in Figure 2. Figure 6 shows that for 100,000 time steps in the fluid for 150,000 time steps in the solid total discrete energy is very well conserved, as in the case of p/q = 1/2 in Figure 3.

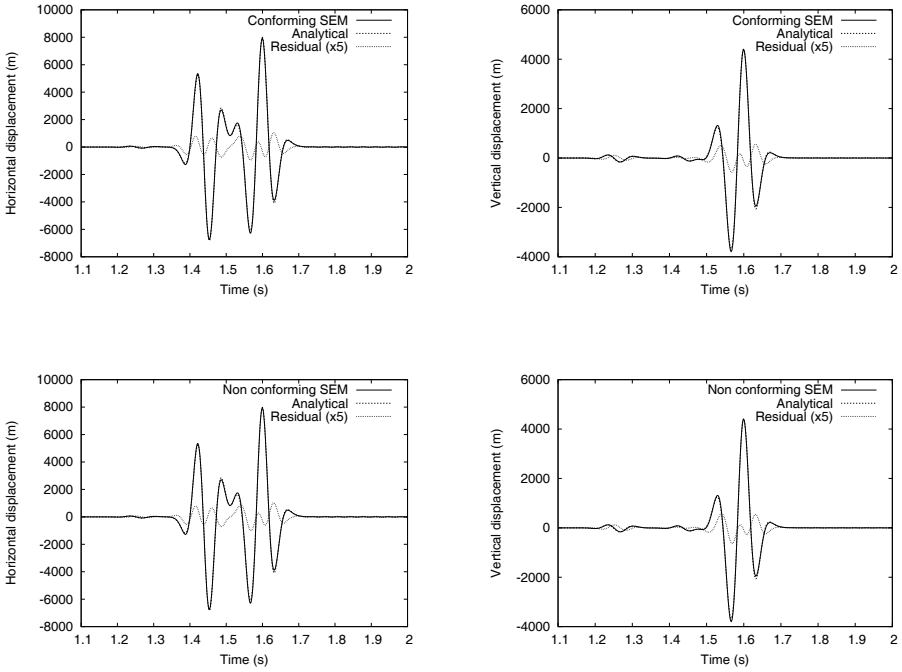

Figure 4: Comparison with the analytical solution from Berg, If, Nielsen, and Skovegaard (1994) (dashed line) of spectral-element seismograms (solid line) for the horizontal (left) and vertical (right) components of the displacement vector at the receiver located in the fluid. The difference amplified by a factor of 5 is also shown (dotted line). (Top) The fit is not very good for conforming time stepping with $\Delta t_f = \Delta t_s = 1.125$ ms, i.e., at about CFL/2 in the fluid and CFL in the solid. (Bottom) The fit is also not very good for non-conforming time stepping with $\Delta t_f = 1.125$ ms in the fluid and $\Delta t_s = 0.5625$ ms in the solid, i.e., at about CFL/2 in both the fluid and the solid.

4.2 Sinusoidal interface with $\Delta t_s = \Delta t_f/2$

Let us see if our time substepping scheme is still stable and accurate in the case of a fluid-solid interface with a more complex shape. Again, we select the same mesh and model as in Komatitsch, Barnes, and Tromp (2000), but will introduce time substepping. The size of the mesh, number of spectral elements in the mesh, and the properties of the model remain unchanged compared to the previous section but the fluid-solid interface (the ocean bottom) now has a sinusoidal shape, as illustrated in Figure 7. The source is located at $x_s = 2908.33$ m at a depth of $z_s = 1700$ m below the free surface of the fluid, and the receiver is located at $x_r = 4053.06$ m at a depth

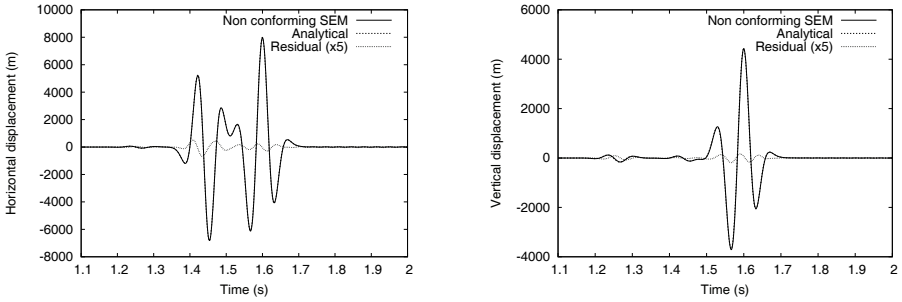

Figure 5: Comparison with the analytical solution from Berg, If, Nielsen, and Skovegaard (1994) (dashed line) of the spectral-element seismogram (solid line) for the horizontal (left) and vertical (right) components of the displacement vector at the receiver located in the fluid. The difference amplified by a factor of 5 is also shown (dotted line). The fit is excellent for non-conforming time stepping with a ratio p/q = 2/3, with $\Delta t_f = 0.42$ ms in the fluid and $\Delta t_s = 0.28$ ms in the solid, i.e., at about CFL/5 in the fluid and CFL/4 in the solid.

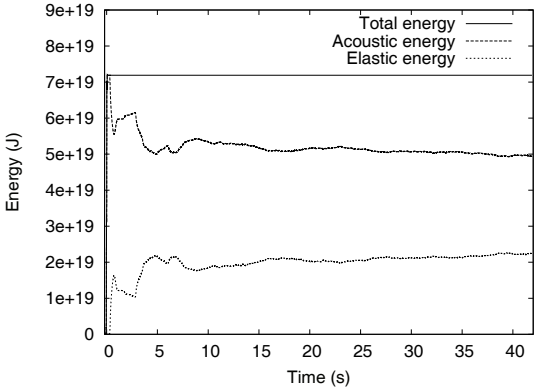

Figure 6: Time evolution of discrete energy in the fluid and in the solid as well as total discrete energy for the non conforming case with p/q = 2/3 for the model with a flat fluid-solid interface. We have $2\Delta t_f = 3\Delta t_s = 0.84$ ms. We propagate the wave field for 100,000 time steps in the fluid for 150,000 time steps in the solid. Total discrete energy is very well conserved.

of $z_r = 1500$ m.

Since there is no known analytical solution in the case of a sinusoidal interface, let us compare the spectral-element solution with conforming time stepping to the spectral-element solution with time substepping for a p/q ratio of 1/2, i.e., for $\Delta t_s = \Delta t_f/2$. In Figure 8 we compare the seismograms for the two components of the displacement vector at the receiver for the conforming case with $\Delta t_f = \Delta t_s = 0.7$ ms and the non conforming case with $\Delta t_f = 2\Delta t_s = 0.7$ ms. The fit obtained is excellent. Figure 9 illustrates the fact that total discrete energy remains approximately constant for 100,000 time steps in the fluid and 200,000 time steps in the solid.

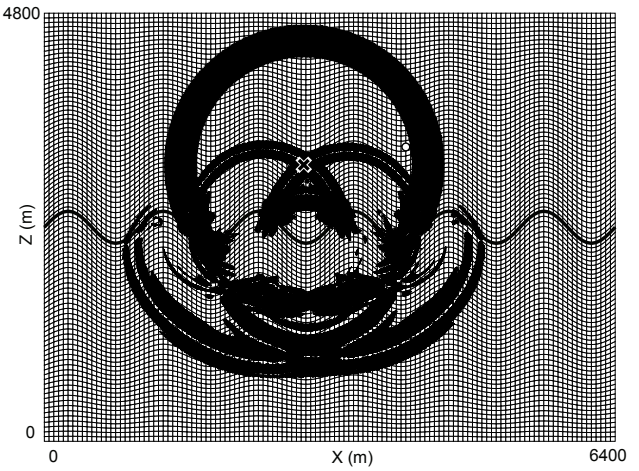

Figure 7: Mesh used for a sinusoidal ocean bottom with free surfaces on the four sides of the grid. The snapshot of the wave field superimposed is shown at time $t = 1.0493$ s and shows the pressure waves in the fluid upper layer and the pressure and shear waves in the solid lower layer. The mesh is the same as in Komatitsch, Barnes, and Tromp (2000). The cross represents the position of the source and the circle indicates the position of the seismic receiver.

5 Analysis of cost reduction

Let us now analyze how the cost (in terms of the total number of calculations to perform) is reduced when resorting to the time substepping technique that we have introduced compared to when using a conforming method in time. For the sake of simplicity let us assume that, as in Figure 1, we have a fluid and a solid layer in contact through a horizontal interface, and that the 2D mesh is topologically regular and composed of NX spectral elements in the horizontal direction, NZ_f spectral

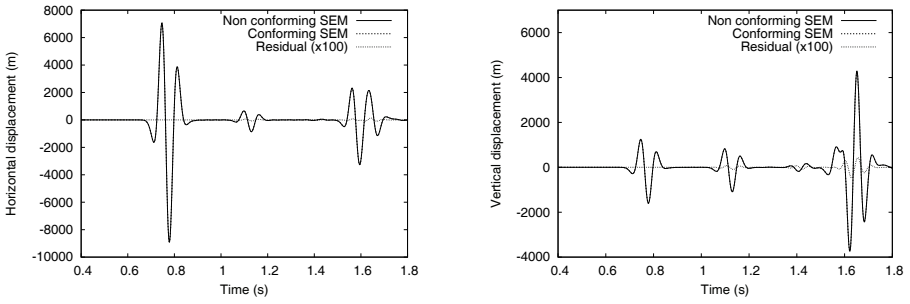

Figure 8: Comparison of spectral-element seismograms for the horizontal (left) and vertical (right) components of the displacement vector at the receiver located in the fluid for the model with sinusoidal bathymetry. The fit is excellent between non-conforming time stepping (solid line) with $\Delta t_f = 2\Delta t_s = 0.7$ ms (i.e., p/q = 1/2) and conforming time stepping (dashed line) with $\Delta t_f = \Delta t_s = 0.7$ ms. The difference amplified by a factor of 100 is also shown (dotted line).

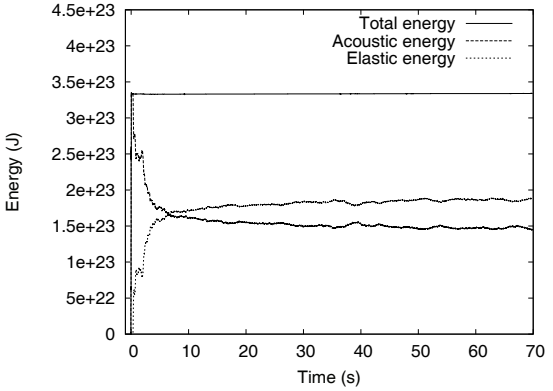

Figure 9: Time evolution of discrete energy in the fluid and in the solid as well as total discrete energy for the non conforming case with p/q = 1/2 for the model with sinusoidal bathymetry. We have $\Delta t_f = 2\Delta t_s = 0.7$ ms. We propagate the wave field for 100,000 time steps in the fluid for 200,000 time steps in the solid. Total discrete energy is very well conserved.

elements in the vertical direction in the fluid layer, and NZ_s spectral elements in the vertical direction in the solid layer. The number of spectral-element edges along the fluid-solid interface is therefore also NX. Let us use a polynomial degree N for the Lagrange interpolants, i.e., a given spectral element contains $\mathrm{NGLL} = \mathrm{N}+1$ Gauss-Lobatto-Legendre in each spatial direction. The total number of points in the fluid layer is then

$$n_f = (\mathrm{NX}\,\mathrm{N}+1)(\mathrm{NZ}_f\,\mathrm{N}+1)\,, \tag{25}$$

the total number of points in the solid layer is

$$n_s = (\mathrm{NX}\,\mathrm{N}+1)(\mathrm{NZ}_s\,\mathrm{N}+1)\,, \tag{26}$$

and the total number of points along the fluid-solid coupling interface is

$$n_{\mathrm{interface}} = \mathrm{NX}\,\mathrm{N}+1\,. \tag{27}$$

The number of points to update on the fluid side to implement the coupling with a $p/q < 1$ substepping ratio is therefore

$$n_f^{\mathrm{coupling}} = (\mathrm{NX}\,\mathrm{N}+1)((q-1)\,\mathrm{N}+1) \tag{28}$$

and the number of points to update on the solid side to implement the coupling is

$$n_s^{\mathrm{coupling}} = (\mathrm{NX}\,\mathrm{N}+1)((p-1)\,\mathrm{N}+1)\,. \tag{29}$$

When one counts the total number of operations that must be performed at each time step in the SEM algorithm, one can show that the total number of operations in the fluid is

$$f_f(\mathrm{NX},\mathrm{NZ}_f) = 9\,n_f + \mathrm{NX}\times\mathrm{NZ}_f(10\,\mathrm{NGLL}^3 + 18\,\mathrm{NGLL}^2) + 13\,\mathrm{NX}\times\mathrm{NGLL} \tag{30}$$

and that the total number of operations in the solid is

$$f_s(\mathrm{NX},\mathrm{NZ}_s) = 18\,n_s + \mathrm{NX}\times\mathrm{NZ}_s(16\,\mathrm{NGLL}^3 + 40\,\mathrm{NGLL}^2) + 13\,\mathrm{NX}\times\mathrm{NGLL}\,. \tag{31}$$

The additional number of operations required to solve the LU linear system and therefore implement the p/q substepping is

$$\begin{aligned} f_{\mathrm{coupling}}(\mathrm{NX}) &= 29\,n_{\mathrm{interface}} + 2\,n_{\mathrm{interface}}^2 + 12(q-1)n_s^{\mathrm{coupling}} \\ &+ \mathrm{NX}(q-1)(16\,\mathrm{NGLL}^3 + 40\,\mathrm{NGLL}^2) + 13q\times\mathrm{NX}\times\mathrm{NGLL} \\ &+ 6q\times n_s^{\mathrm{coupling}} + 6(p-1)n_f^{\mathrm{coupling}} \\ &+ \mathrm{NX}(p-1)(10\,\mathrm{NGLL}^3 + 18\,\mathrm{NGLL}^2) \\ &+ 13p\times\mathrm{NX}\times\mathrm{NGLL} + 3n_f^{\mathrm{coupling}} + 6n_s^{\mathrm{coupling}} + 3n_f^{\mathrm{coupling}}\,. \end{aligned} \tag{32}$$

As a result, the gain that we obtain by resorting to p/q substepping compared to a conforming approach with no substepping is

$$\text{gain}(\text{NX}, \text{NZ}_f, \text{NZ}_s) = \frac{q \times (f_f(\text{NX}, \text{NZ}_f) + f_s(\text{NX}, \text{NZ}_s))}{p \times f_f(\text{NX}, \text{NZ}_f) + q \times f_s(\text{NX}, \text{NZ}_s) + f_{\text{coupling}}(\text{NX})} . \tag{33}$$

In Figure 10 we show that gain as a function of NX for p/q = 1/2 for an ocean acoustics simulation is which we have a deep ocean layer and a thinner solid layer to represent the coupling at the ocean bottom. The fluid layer occupies 80% of the whole domain in the vertical direction, the solid layer 20%, and we take NX = $(\text{NZ}_f + \text{NZ}_s) \times 4/3$, i.e., the model is slightly elongated in the horizontal direction as in Figures 1 and 7, which is often the case in oil industry or ocean acoustics geophysical models. One can see that we save a factor of about 1.5 in terms of the total number of operations when resorting to time substepping.

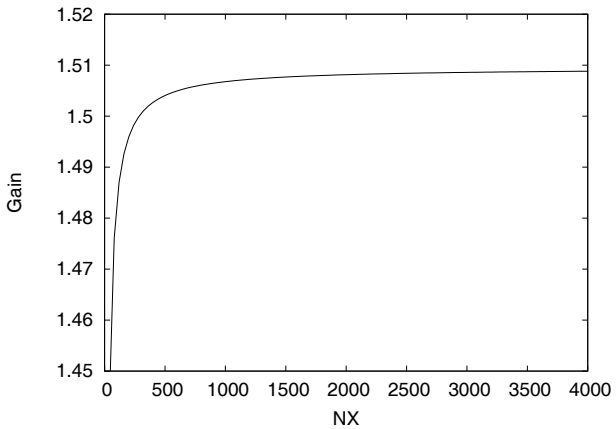

Figure 10: Gain as a function of the number of spectral-element edges along the fluid-solid interface (NX) for a time substepping ratio p/q = 1/2 for an ocean acoustics simulation is which we have a deep ocean layer and a thinner solid layer to represent the coupling at the ocean bottom. The fluid layer occupies 80% of the whole domain in the vertical direction, the solid layer 20%, and we take NX = $(\text{NZ}_f + \text{NZ}_s) \times 4/3$, i.e., the model is slightly elongated in the horizontal direction, which is often the case in oil industry or ocean acoustics geophysical models. We save a factor of about 1.5 in terms of the total number of operations by resorting to time substepping.

6 Conclusions and future work

We have introduced a time substepping technique that enforces the conservation of energy along the fluid-solid interface for seismic wave propagation in fluid-solid models and implemented it in the context of an explicit conditionally-stable Newmark finite-difference time scheme. Using time substepping is often of interest for seismic wave propagation modeling because the stability condition in the solid part of the medium can lead to a significantly smaller time step than in the fluid. To enforce conservation of energy along the fluid-solid interface we need to solve a linear system along the fluid-solid interface. This system does not change with time and can therefore be decomposed once and for all before the time loop.

Numerical tests performed based on a spectral-element method (SEM) have shown that energy conservation along the fluid-solid interface is ensured; therefore the method remains stable even for very long simulations of 200,000 time steps. However the Newmark time-integration scheme used in the classical SEM (independently of fluid-solid coupling or time substepping) is not very accurate compared to the high order of the spatial approximation, therefore the accuracy decreases when one approaches the CFL stability limit because of numerical dispersion in the time scheme on the fluid side (which usually has the largest time step because of a lower maximum pressure wave speed). Therefore in the future higher-order time schemes such as fourth-order Runge-Kutta or symplectic schemes (Simo, Tarnow, and Wong, 1992; Tarnow and Simo, 1994; Nissen-Meyer, Fournier, and Dahlen, 2008; Celledoni, McLachlan, McLaren, Owren, Quispel, and Wright, 2009) should be used. Because the mass matrix is diagonal such an extension should not be too difficult to implement.

Future work could also include using a more complex rheology in the solid, for instance poroelastic (e.g., Ezziani, 2006; Martin, Komatitsch, and Ezziani, 2008), as well as adding optimized Convolutional Perfectly Matched Layers (CPMLs) in the fluid and in the solid (Komatitsch and Martin, 2007) to absorb outgoing waves on the fictitious edges of the grid. Let us note that CPML is compatible with complex rheologies such as poroelastic media (Martin, Komatitsch, and Ezziani, 2008) and can be adapted to variational methods (Martin, Komatitsch, and Gedney, 2008).

Coupling this technique with a spatially non-conforming mesh at the fluid-solid interface for instance using the 'mortar' method (Chaljub, Capdeville, and Vilotte, 2003) or conservative load transfer (Jaiman, Jiao, Geubelle, and Loth, 2006) could also be of interest in some cases, although in many cases of practical interest, for instance in the oil industry, the value of the shear wave velocity at the ocean bottom on the solid side is similar to the value of the pressure wave velocity on the fluid side (in the ocean) and thus a spatially-conforming mesh is needed to keep a similar

mesh resolution.

Extension to 3D, although straightforward because the time substepping formulation presented does not depend on the spatial dimension of the problem, should be implemented. To solve the linear system on the fluid-solid interface to enforce conservation of energy there, one could still build its LU decomposition once and for all before the time loop. In the case of 3D simulations, it is often inevitable to use a parallel computer because of the large size of the mesh. One should then use a parallel solver such as MUMPS (Amestoy, Duff, Koster, and L'Excellent, 2001) or PaStiX (Hénon and Saad, 2006), in which the LU decomposition and storage is optimized for large parallel computers.

The time substepping technique introduced for a fluid-solid model and the matrix systems presented can also be used in any other numerical method that has a diagonal mass matrix, such as discontinuous Galerkin techniques (e.g., Bernacki, Lanteri, and Piperno (2006); Käser and Dumbser (2006)) or finite elements with mass lumping (e.g., Diaz and Joly (2005)).

Acknowledgement: The authors would like to thank an anonymous reviewer and the associate editor for comments that improved the manuscript. Ronan Madec and Dimitri Komatitsch thank Pierre Thore and TOTAL MTS/INNO for financial support.

References

Alterman, Z.; Karal, F. C. (1968): Propagation of elastic waves in layered media by finite difference methods. *Bull. Seismol. Soc. Am.*, vol. 58, pp. 367–398.

Amestoy, P. R.; Duff, I. S.; Koster, J.; L'Excellent, J.-Y. (2001): A fully asynchronous multifrontal solver using distributed dynamic scheduling. *SIAM Journal on Matrix Analysis and Applications*, vol. 23, no. 1, pp. 15–41.

Berg, P.; If, F.; Nielsen, P.; Skovegaard, O. (1994): Analytic reference solutions. In Helbig, K.(Ed): *Modeling the Earth for oil exploration, Final report of the CEC's GEOSCIENCE I Program 1990-1993*, pp. 421–427. Pergamon Press, Oxford, United Kingdom.

Bernacki, M.; Lanteri, S.; Piperno, S. (2006): Time-domain parallel simulation of heterogeneous wave propagation on unstructured grids using explicit, nondiffusive, discontinuous Galerkin methods. *J. Comput. Acoust.*, vol. 14, no. 1, pp. 57–81.

Bielak, J.; Ghattas, O.; Kim, E. J. (2005): Parallel octree-based finite element method for large-scale earthquake ground motion simulation. *CMES: Computer Modeling in Engineering and Science*, vol. 10, no. 2, pp. 99–112.

Carcione, J. M. (1994): The wave equation in generalized coordinates. *Geophysics*, vol. 59, pp. 1911–1919.

Casadei, F.; Halleux, J.-P. (2009): Binary spatial partitioning of the central-difference time integration scheme for explicit fast transient dynamics. *Int. J. Numer. Meth. Eng.*, vol. 78, no. 12, pp. 1436–1473.

Celledoni, E.; McLachlan, R. I.; McLaren, D. I.; Owren, B.; Quispel, G. R. W.; Wright, W. M. (2009): Energy-preserving Runge-Kutta methods. *M2AN*, vol. 43, pp. 645–649.

Chaljub, E.; Capdeville, Y.; Vilotte, J. P. (2003): Solving elastodynamics in a fluid-solid heterogeneous sphere: a parallel spectral-element approximation on non-conforming grids. *J. Comput. Phys.*, vol. 187, no. 2, pp. 457–491.

Chaljub, E.; Komatitsch, D.; Vilotte, J.-P.; Capdeville, Y.; Valette, B.; Festa, G. (2007): Spectral element analysis in seismology. In Wu, R.-S.; Maupin, V.(Eds): *Advances in Wave Propagation in Heterogeneous Media*, volume 48 of *Advances in Geophysics*, pp. 365–419. Elsevier - Academic Press.

Cohen, G. (2002): *Higher-order numerical methods for transient wave equations*. Springer-Verlag, Berlin, Germany.

Collino, F.; Fouquet, T.; Joly, P. (2003): A conservative space-time mesh refinement method for the 1-D wave equation. I. Construction. *Numerische Mathematik*, vol. 95, no. 2, pp. 197–221.

Collino, F.; Fouquet, T.; Joly, P. (2003): A conservative space-time mesh refinement method for the 1-D wave equation. II. Analysis. *Numerische Mathematik*, vol. 95, no. 2, pp. 223–251.

De Basabe, J. D.; Sen, M. K. (2007): Grid dispersion and stability criteria of some common finite-element methods for acoustic and elastic wave equations. *Geophysics*, vol. 72, no. 6, pp. T81–T95.

Diaz, J.; Grote, M. J. (2009): Energy conserving explicit local time stepping for second-order wave equations. *SIAM J. Sci. Comput.*, vol. 31, no. 3, pp. 1985–2014.

Diaz, J.; Joly, P. (2005): A robust high-order non-conforming finite-element formulation for time domain fluid-structure interaction. *J. Comput. Acoust.*, vol. 13, no. 3, pp. 403–431.

Dumbser, M.; Käser, M.; Toro, E. (2007): An arbitrary high-order discontinuous Galerkin method for elastic waves on unstructured meshes, Part V: Local time stepping and *p*-adaptivity. *Geophys. J. Int.*, vol. 171, no. 2, pp. 695–717.

El Soueidy, C. P.; Younes, A.; Ackerer, P. (2009): Solving the advection-diffusion equation on unstructured meshes with discontinuous/mixed finite elements and a local time stepping procedure. *Int. J. Numer. Meth. Eng.*, vol. 79, no. 9, pp. 1068–1093.

Ezziani, A. (2006): Ondes dans les milieux poroélastiques : analyse du modèle de Biot. *Revue Africaine de la Recherche en Informatique et Mathématiques Appliquées ARIMA*, vol. 5, pp. 95–109.

Fauqueux, S. (2003): *Eléments finis mixtes spectraux et couches absorbantes parfaitement adaptées pour la propagation d'ondes élastiques en régime transitoire*. PhD thesis, Université Paris-Dauphine, Paris, France, 2003.

Hairer, E.; Lubich, C.; Wanner, G. (2006): *Geometric numerical integration*, volume 31 of *Springer Series in Computational Mathematics*. Springer-Verlag, Berlin, Germany, second edition.

Hénon, P.; Saad, Y. (2006): A parallel multistage ILU factorization based on a hierarchical graph decomposition. *SIAM Journal of Scientific Computing*, vol. 28, no. 6, pp. 2266–2293.

Hughes, T. J. R. (1987): *The finite element method, linear static and dynamic finite element analysis*. Prentice-Hall International, Englewood Cliffs, New Jersey, USA.

Jaiman, R. K.; Jiao, X.; Geubelle, P. H.; Loth, E. (2006): Conservative load transfer along curved fluid-solid interface with non-matching meshes. *J. Comput. Phys.*, vol. 218, no. 1, pp. 372–397.

Kane, C.; Marsden, J. E.; Ortiz, M.; West, M. (2003): Variational integrators and the Newmark algorithm for conservative and dissipative mechanical systems. *Int. J. Numer. Meth. Eng.*, vol. 49, no. 10, pp. 1295–1325.

Kang, T.-S.; Baag, C.-E. (2004): Finite-difference seismic simulation combining discontinuous grids with locally variable timesteps. *Bull. Seismol. Soc. Am.*, vol. 94, no. 1, pp. 207–219.

Käser, M.; Dumbser, M. (2006): An arbitrary high-order discontinuous Galerkin method for elastic waves on unstructured meshes-I. The two-dimensional isotropic case with external source terms. *Geophys. J. Int.*, vol. 166, no. 2, pp. 855–877.

Käser, M.; Dumbser, M. (2008): A highly accurate discontinuous Galerkin method for complex interfaces between solids and moving fluids. *Geophysics*, vol. 73, no. 3, pp. T23–T35.

Kawase, H. (1988): Time-domain response of a semi-circular canyon for incident *SV*, *P* and Rayleigh waves calculated by the discrete wavenumber boundary element method. *Bull. Seismol. Soc. Am.*, vol. 78, pp. 1415–1437.

Komatitsch, D.; Barnes, C.; Tromp, J. (2000): Wave propagation near a fluid-solid interface: a spectral element approach. *Geophysics*, vol. 65, no. 2, pp. 623–631.

Komatitsch, D.; Martin, R. (2007): An unsplit convolutional Perfectly Matched Layer improved at grazing incidence for the seismic wave equation. *Geophysics*, vol. 72, no. 5, pp. SM155–SM167.

Komatitsch, D.; Tromp, J. (2002): Spectral-element simulations of global seismic wave propagation-I. Validation. *Geophys. J. Int.*, vol. 149, no. 2, pp. 390–412.

Komatitsch, D.; Vilotte, J. P. (1998): The spectral-element method: an efficient tool to simulate the seismic response of 2D and 3D geological structures. *Bull. Seismol. Soc. Am.*, vol. 88, no. 2, pp. 368–392.

Krenk, S. (2006): Energy conservation in Newmark based time integration algorithms. *Comput. Meth. Appl. Mech. Eng.*, pp. 6110–6124.

Liu, Q.; Polet, J.; Komatitsch, D.; Tromp, J. (2004): Spectral-element moment tensor inversions for earthquakes in Southern California. *Bull. Seismol. Soc. Am.*, vol. 94, no. 5, pp. 1748–1761.

Lysmer, J.; Drake, L. A. (1972): A finite element method for seismology. In Alder, B.; Fernbach, S.; Bolt, B. A.(Eds): *Methods in Computational Physics*, volume 11, chapter 6, pp. 181–216. Academic Press, New York, USA.

Madariaga, R. (1976): Dynamics of an expanding circular fault. *Bull. Seismol. Soc. Am.*, vol. 66, no. 3, pp. 639–666.

Martin, R.; Komatitsch, D.; Ezziani, A. (2008): An unsplit convolutional perfectly matched layer improved at grazing incidence for seismic wave equation in poroelastic media. *Geophysics*, vol. 73, no. 4, pp. T51–T61.

Martin, R.; Komatitsch, D.; Gedney, S. D. (2008): A variational formulation of a stabilized unsplit convolutional perfectly matched layer for the isotropic or anisotropic seismic wave equation. *CMES: Computer Modeling in Engineering and Science*, vol. 37, no. 3, pp. 274–304.

Newmark, N. M. (1959): A method of computation for structural dynamics. In *Engineering mechanics division: Proceedings of the American Society of Civil Engineers*, pp. 67–93.

Nissen-Meyer, T.; Fournier, A.; Dahlen, F. A. (2008): A 2-D spectral-element method for computing spherical-earth seismograms - II. Waves in solid-fluid media. *Geophys. J. Int.*, vol. 174, pp. 873–888.

Rodríguez, J. (2004): *Raffinement de maillage spatio-temporel pour les équations de l'élastodynamique*. PhD thesis, Université Paris IX-Dauphine, Paris, France, 2004.

Sánchez-Sesma, F. J.; Campillo, M. (1991): Diffraction of *P*, *SV* and Rayleigh waves by topographic features: a boundary integral formulation. *Bull. Seismol. Soc. Am.*, vol. 81, pp. 2234–2253.

Seriani, G.; Oliveira, S. P. (2008): Dispersion analysis of spectral-element methods for elastic wave propagation. *Wave Motion*, vol. 45, pp. 729–744.

Simo, J. C.; Tarnow, N.; Wong, K. K. (1992): Exact energy-momentum conserving algorithms and symplectic schemes for nonlinear dynamics. *Comput. Meth. Appl. Mech. Eng.*, vol. 100, pp. 63–116.

Soares Jr., D. (2009): Acoustic modelling by BEM-FEM coupling procedures taking into account explicit and implicit multi-domain decomposition techniques. *Int. J. Numer. Meth. Eng.*, vol. 78, no. 9, pp. 1076–1093.

Soares Jr., D.; Mansur, W. J. (2005): An efficient time-domain BEM-FEM coupling for acoustic-elastodynamic interaction problems. *CMES: Computer Modeling in Engineering and Science*, vol. 8, no. 2, pp. 153–164.

Soares Jr., D.; Mansur, W. J.; Lima, D. L. (2007): An explicit multi-level time-step algorithm to model the propagation of interacting acoustic-elastic waves using finite-element/finite-difference coupled procedures. *CMES: Computer Modeling in Engineering and Science*, vol. 17, no. 1, pp. 19–34.

Tarnow, N.; Simo, J. C. (1994): How to render second-order accurate time-stepping algorithms fourth-order accurate while retaining the stability and conservation properties. *Comput. Meth. Appl. Mech. Eng.*, vol. 115, pp. 233–252.

Tessmer, E. (2000): Seismic finite-difference modeling with spatially varying time steps. *Geophysics*, vol. 65, no. 4, pp. 1290–1293.

Tessmer, E.; Kosloff, D. (1994): 3-D elastic modeling with surface topography by a Chebyshev spectral method. *Geophysics*, vol. 59, no. 3, pp. 464–473.

van Vossen, R.; Robertsson, J. O. A.; Chapman, C. H. (2002): Finite-difference modeling of wave propagation in a fluid-solid configuration. *Geophysics*, vol. 67, no. 2, pp. 618–624.

Virieux, J. (1986): *P-SV* wave propagation in heterogeneous media: velocity-stress finite-difference method. *Geophysics*, vol. 51, pp. 889–901.

Zhang, J. (2004): Wave propagation across fluid-solid interfaces: a grid method approach. *Geophys. J. Int.*, vol. 159, no. 1, pp. 240–252.